Octahedral Void Structure Observed in Grown-In Defects in the Bulk of Standard Czochralski-Si for MOS LSIs

Jpn. J. Appl. Phys. Vol. 36 (1997) pp. 1781–1785
Part 1, No. 3B, March 1997

Octahedral Void Structure Observed in Grown-In Defects in the Bulk of Standard Czochralski-Si for MOS LSIs

Takemi UEKI, Manabu ITSUMI[1] and Tadao TAKEDA[1]

NTT Electronics Technology Corp., Atsugi-Shi, Kanagawa Pref. 243-01, Japan
[1]*System Electronics Laboratories, NTT, Atsugi-Shi, Kanagawa Pref. 243-01, Japan*

(Received September 24, 1996; accepted for publication November 22, 1996)

We analyzed the structure of octahedral voids in the bulk of standard silicon wafers. They are often twin type and are about 100 nm in size. The structure of the defect is incompletely octahedron, and is mainly surrounded by {111} planes. Our electron diffraction and energy-dispersive X-ray spectroscopy analyses suggest that the octahedron defect is void. A 2-nm-thick layer exists on each of the side walls of the void defect. Our auger electron spectroscopy analysis suggests that the 2-nm-thick layer is SiO_2. It is believed that the void structure is formed during Si-ingot growth.

KEYWORDS: Czochralski-Si, grown-in defect, LSTD, TEM, ED-pattern, EDS, AES

1. Introduction

Gate oxide defects act as so-called B-mode defects, and are a major factor influencing the yield and reliability of metal-oxide-semiconductor (MOS) LSIs. Figure 1 shows the defect density of gate-oxide film measured by the breakdown voltage of MOS diodes. The defect density of oxides thermally grown on Czochralski silicon (CZ-Si) is clearly larger than that of oxides thermally grown on float-zone silicon (FZ-Si). The origin of the oxide defects may be the grown-in defects (microdefects) in CZ-Si.[1)] These include oxygen precipitates,[2)] crystal originated particles (COP) after SC1 cleaning,[3)] flow-pattern defects (FPD) after Secco etching[4)] and laser scattering tomography defects (LSTD)[5)] detected by infrared (IR) laser. Analysis of the defect by secondary ion mass spectrometry (SIMS) detected oxygen from the grown-in defect.[6)] Moreover, EDS analysis using a transmission electron microscope (TEM) also detected oxygen in the grown-in defect.[7)] These results are from the analysis of the surface, Thus the cross-sectional structure is yet unidentified. Until now, analysis of a low density of defects (about $10^6\,cm^{-3}$) has been difficult.

In recent studies, copper decoration followed by focus ion beam (FIB) thinning of samples revealed an octahedral void structure just beneath the oxide defects.[8–10)] These results suggest that the octahedron defect is a void. This observation is based on the copper decoration, which might have some influence on the defect structure. In this study, we observed the grown-in defect directly, without the influence of copper decoration.

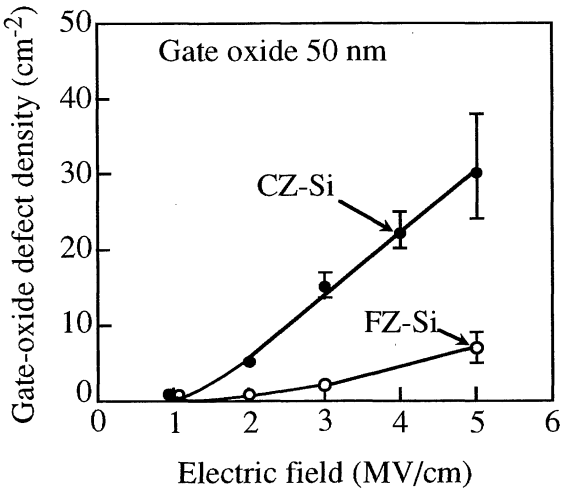

Fig. 1. Comparison of CZ-Si and FZ-Si wafers.

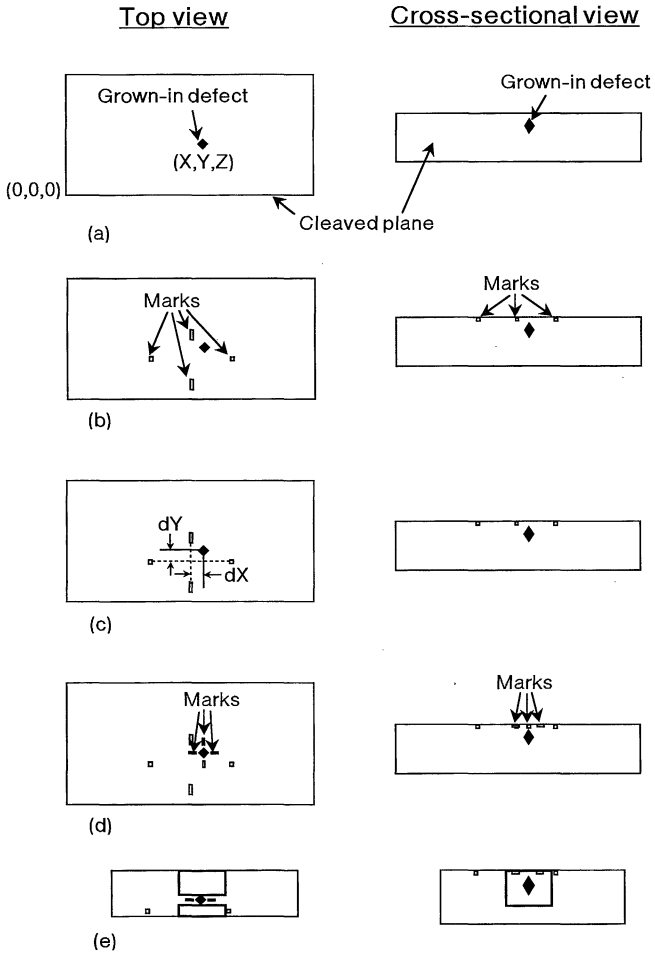

Fig. 2. Preparation method of observation specimen: (a) the first coordinate measurement by IR-tomography, (b) the first marking by FIB, (c) the second coordinate measurement by IR-tomography, (d) the second marking by FIB and (e) thinning by FIB.

2. Experimental

The wafers used were 6-inch-diameter (100)-oriented boron-doped standard CZ-Si wafers. Oxygen concentration in the substrates was 13.8–14.5 $\times$ 10^{17} atoms/cm^3 (ASTM79). The specimen preparation procedure is outlined in Fig. 2, which shows the top and cross-sectional views. First, the wafers were cleaved to form specimens. Then, we measured three-dimensional coordinates using Mitsui MO-401 IR-tomography (Fig. 2(a)). We used four dots to mark the area surrounding the defect (Fig. 2(b)) with FIB (Seiko Inst., SMI-8400SE), which had a Gallium-ion beam of 30 keV. Next, the arrangement of the four dots was reconfirmed using IR-tomography (Fig. 2(c)), since this gave us the distance of a defect and the first time marks. We then processed the four marks by FIB once again (Fig. 2(d)) in order to form a guide from which the TEM specimen was prepared. After that, the specimens were cut out using a diamond saw. Finally, the FIB thinning and TEM (Hitachi, HF-2000) observations were repeated a few times so that the defects might be included in the specimen (Fig. 2(e)). The specimens were thinned by FIB to about 300 nm for TEM observation. The success rate of our specimen preparation method was about 50%.

The specimens were analyzed using energy-dispersive X-ray spectroscopy (EDS: Kevex, Delta system). Analysis by auger electron spectroscopy (AES: Physical electronics, Model-670) with a more precise detection limit was also done using Ar sputtering.

3. Results and Discussion

3.1 *TEM observation*

A cross-sectional TEM image of a typical grown-in de-

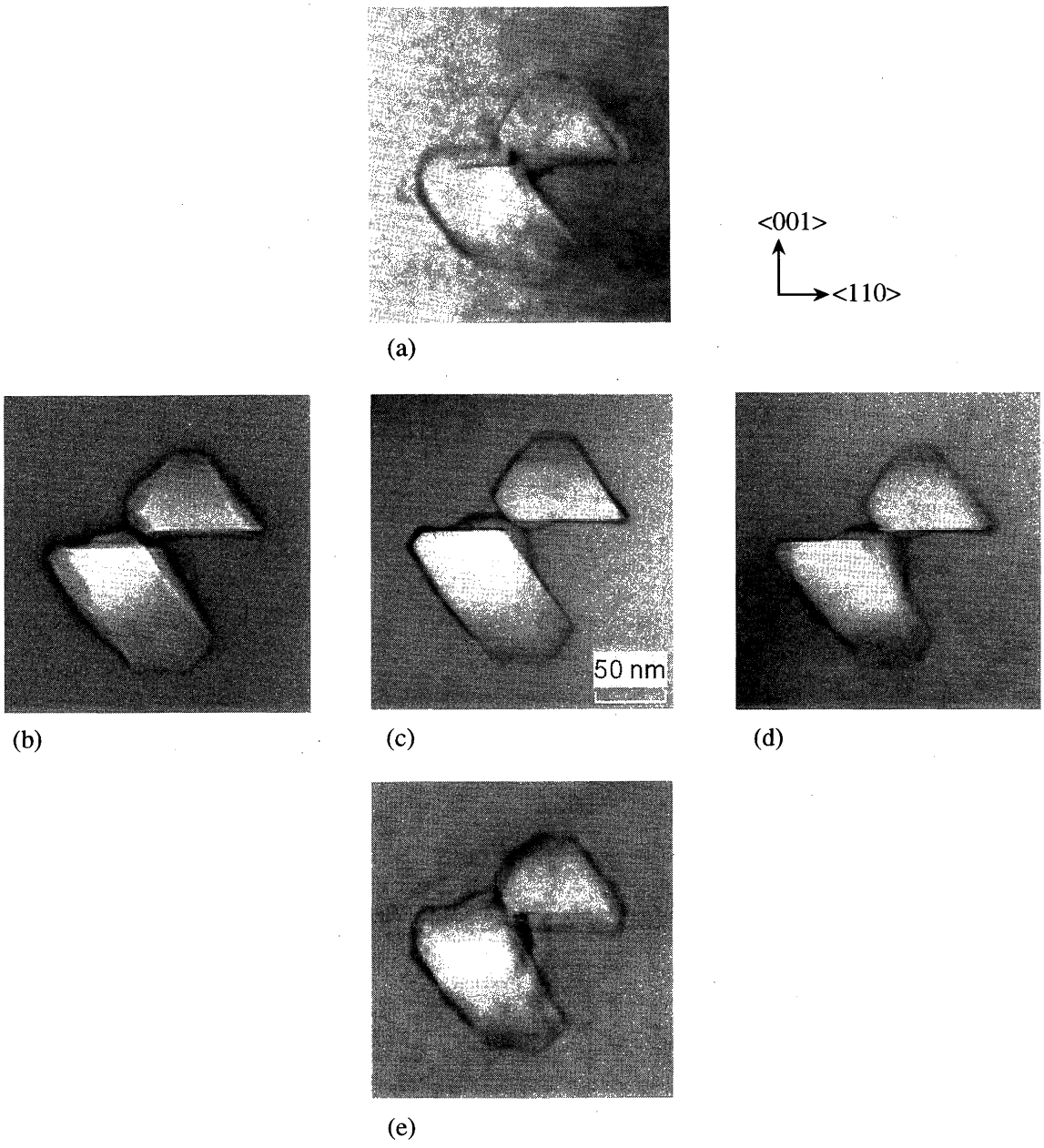

Fig. 3. Cross-sectional TEM observation of the grown-in defect structure: (a) +15° tilt to the ⟨001⟩ plane, (b) −15° tilt to the ⟨110⟩ plane, (c) no tilt, (d) +15° tilt to the ⟨110⟩ plane and (e) −15° tilt to the ⟨001⟩ plane.

fect is shown in Fig. 3. Each angle tilt was +15° and −15° to the ⟨001⟩ and ⟨110⟩ plane. The defects are twin-type octahedral defects, about 100 nm in size. The results show that a defect is surrounded by the {111} and {100} plane. Figure 4 illustrates the octahedron defect structure that was estimated from the result in Fig. 3. The structure of the defect is incompletely octahedron, and is mainly surrounded by {111} planes. These features were common for the five TEM images that were obtained. Magnification of the image revealed the existence of a 2-nm-thick layer on the side walls (Fig. 5). A thin layer uniformly covers the side walls. The thickness of this layer is the same for both of the twin defects.

Figure 6 shows the spot locations of the electron diffraction (ED) pattern measurement and the EDS analysis. The beam size of the ED pattern measurement was smaller than the defect size, that is, about 5 nm. Figure 7 shows the ED patterns of an Si matrix (point A in Fig. 6) and twin defects (from point B to point D in Fig. 6).

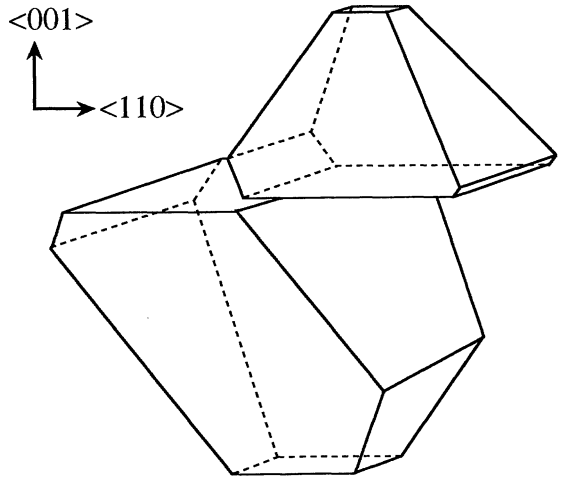

Fig. 4. A schematic illustration of the grown-in defect.

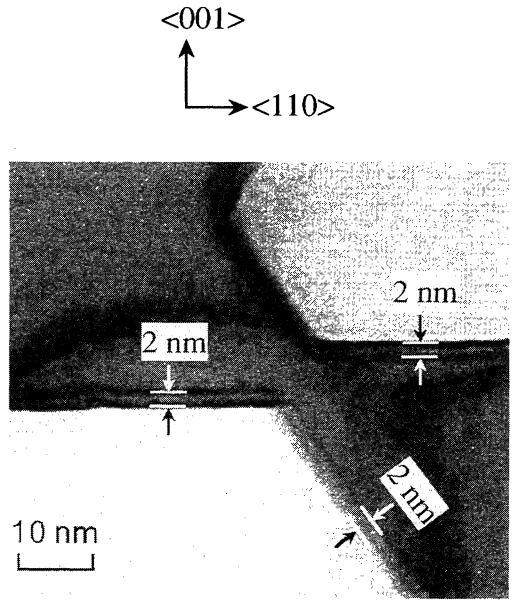

Fig. 5. Side wall structure of the grown-in defect by TEM observation. A 2-nm-thick layer is observed on the side walls.

The ED patterns of the octahedron defects (point B and point D in Fig. 6) and ED pattern of the central part of the twin defects (point C in Fig. 6) were equal to the ED patterns of the Si matrix (point A in Fig. 6), and only diffraction spots of Si bulk were found. If the octahedron defect is filled with crystobalite SiO_2, a ring

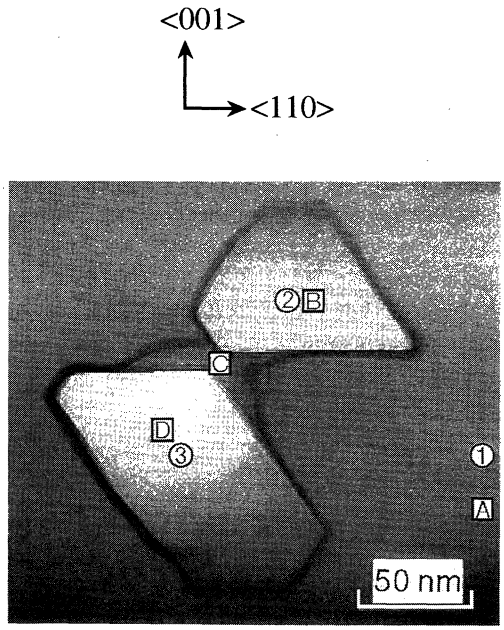

Fig. 6. Measurement points for ED and EDS analysis. From point A to point D: measurement points for ED. From point 1 to point 3: measurement ponts for EDS.

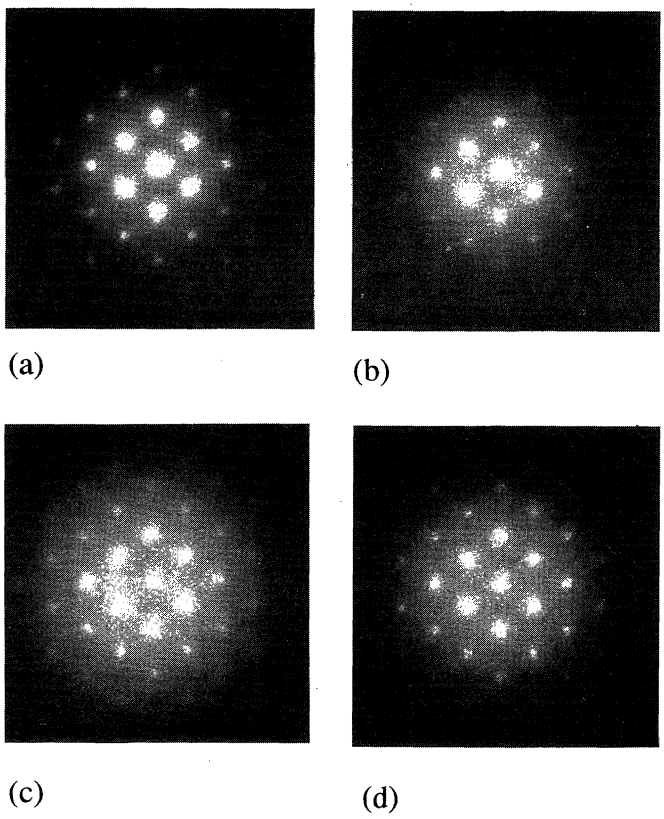

Fig. 7. Electron diffraction pattern of the grown-in defect: (a) point A in Fig. 6, (b) point B in Fig. 6, (c) point C in Fig. 6 and (d) point D in Fig. 6.

pattern appears,[11] and if the octahedron defect is filled with amorphous SiO_2, a halo pattern appears.[12] Neither a ring nor a halo pattern were found in our results, which suggest that the octahedron defect isn't filled with SiO_2.

3.2 *EDS analysis*

EDS spectra (from point 1 to point 3 in Fig. 6) showed that Si was detected, but oxygen wasn't (Fig. 8). If the octahedron defect is filled with SiO_2, oxygen signals should be detected. The intensity of the Si signal for the defect (points 2 and 3 in Fig. 6) was about 30% less than that of the Si signal for the Si matrix (point 1 in Fig. 6). The beam size of the EDS spectra measurement was smaller than the defect size, that is, about 2 nm. These results suggest that the octahedron defect is void.

3.3 *AES analysis*

Figure 9 shows the TEM micrograph of another specimen. Figure 10 shows the AES spectrum when a defect appeared on the surface. Table I shows the intensity change of AES signals by Ar sputtering. The beam size of AES analysis was smaller than the defect size, that is, about 25 nm. AES analysis detected only a signal on the surface. These AES signals were measured after sputtering with Argon until a defect appeared on the surface, or just before it. When a defect (point A in Fig. 9) appeared, the intensity of the oxygen signal increased by about 40%, and the intensity of the Si signal decreased by about 50%. Moreover, a carbon and a copper signal signify contamination of the surface (point A and point B in Fig. 9), and the constant intensity of these signals. AES results revealed that the intensity of the oxygen signal on the surface of the defect (point A in Fig. 9) was larger than that of the oxygen signal for the Si matrix (point B in Fig. 9), suggesting that the 2-nm-thick layer on the side wall was SiO_2.

Table I. The intensity change of the AES signal by Ar sputtering.

Points of analysis	Appearance of surface	Intensity of AES signals (kc/s)		
		Silicon	Oxygen	Carbon
Defect (point A in Fig. 9)	before	879	88	156
	after	443	124	163
Si matrix (point B in Fig. 9)	before	911	78	143
	after	957	75	130

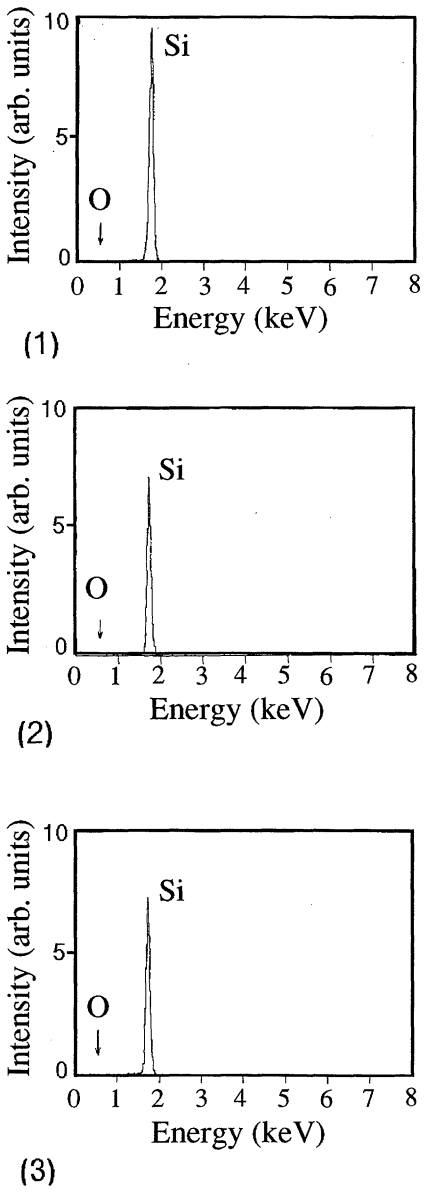

Fig. 8. EDS spectra of the grown-in defect: (1) point 1 in Fig. 6, (2) point 2 in Fig. 6 and (3) point 3 in Fig. 6.

3.4 *Octahedral void structure*

The above results suggests that an octahedral void structure is formed during Si-ingot growth. Agglomeration of vacancies during the Si-ingot growth may result in formation of the void. The structure of the defect is mainly surrounded by {111} planes. The 2-nm-thick

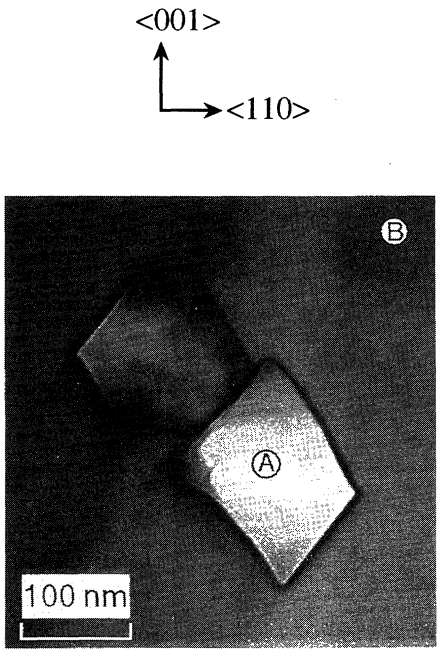

Fig. 9. Measurement points for AES analysis.

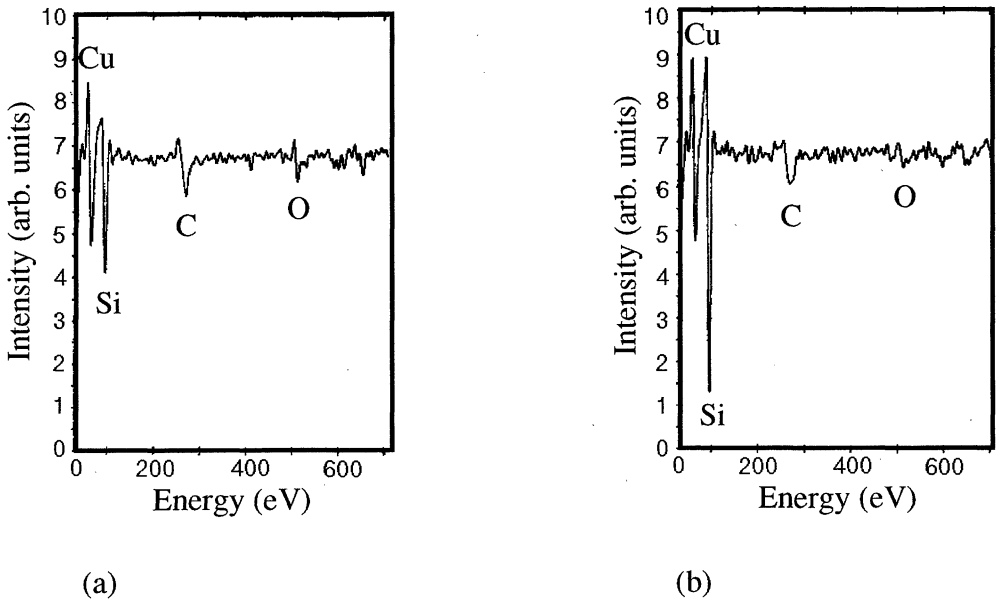

Fig. 10. AES spectra of the grown-in defects: (a) point A in Fig. 9 and (b) point B in Fig. 9.

layer may be formed during the final stage of the formation of the octahedral void structure during the Si-ingot growth. Diffusion and agglomeration of vacancies during the Si-ingot growth should be further investigated experimentally and by simulation.

4. Conclusions

To summarize, we clarified that octahedral void structures with a 2-nm-thick layer were contained in standard as-grown CZ-Si crystals. The structure of the defect was incompletely octahedron, and was mainly surrounded by {111} planes. Results of our ED and EDS analyses suggest that the octahedron defect was void. The thin (2 nm) layer uniformly covered both side walls of the twin defect. Agglomeration of vacancies during the Si-ingot growth may be a possible cause for the void formation. Our AES analysis suggests that the 2-nm-thick layer was SiO_2.

Acknowledgements

The authors are indebted to Dr. Ken Takeya, Dr. Kazuo Imai and Shigeru Nakajima for their continuous encouragement, and to Dr. Kazumi Wada and Dr. Naohisa Inoue of Osaka Furitsu University for important information about gigantic oxygen precipitates and their formation mechanism.

1) M. Itsumi and F. Kiyosumi: Appl. Phys. Lett. **40** (1982) 496.
2) K. Tempelhoff, F. Spiegelberg, R. Gleichmann and D. Wruck: Phys. Stat. Sol. **56** (1979) 213.
3) J. Ryuta, E. Morita, T. Tanaka and Y. Shimanuki: Jpn. J. Appl. Phys. **29** (1990) L1947.
4) H. Yamagishi, I. Fusegawa, N. Fujimaki and M. Katayama: Semicond. Sci. Technol. **7** (1992) A135.
5) S. Umeno, S. Sadamitsu, H. Murakami, M. Hourai, S. Sumita and T. Shigemitsu: Jpn. J. Appl. Phys. **32** (1993) L699.
6) S. Sadamitsu, S. Umeno, Y. Koike, M. Hourai, S. Sumita and T. Shigemitsu: Jpn. J. Appl. Phys. **32** (1993) 3675.
7) M. Miyazaki, S. Miyazaki, Y. Yanase, T. Ochiai and T. Shigemitsu: Jpn. J. Appl. Phys. **34** (1995) 6303.
8) M. Itsumi, M. Tomita and M. Yamawaki: J. Appl. Phys. **78** (1995) 1940.
9) M. Itsumi, H. Akiya, T. Ueki, M. Tomita and M. Yamawaki: J. Appl. Phys. **78** (1995) 5984.
10) M. Itsumi, H. Akiya, T. Ueki, M. Tomita and M. Yamawaki: Jpn. J. Appl. Phys. **35** (1996) 812.
11) K. V. Ravi: J. Electrochem. Soc. **121** (1974) 1090.
12) F. A. Ponce, T. Yamashita and S. Hahn: Appl. Phys. Lett. **43** (1983) 1051.